RAA 2016 Vol. **16** No. **3**, 49 (10pp) doi: 10.1088/1674–4527/16/3/049
http://www.raa-journal.org *http://iopscience.iop.org/raa*

***R**esearch in*
***A**stronomy and*
***A**strophysics*

Imprints of relic gravitational waves on pulsar timing

Ming-Lei Tong[1,2,3], Yong-Heng Ding[1,4], Cheng-Shi Zhao[1,2], Feng Gao[1,4], Bao-Rong Yan[1,5], Ting-Gao Yang[1,2] and Yu-Ping Gao[1,2]

[1] National Time Service Center, Chinese Academy of Sciences, Xi'an 710600, China; *mltong@ntsc.ac.cn*
[2] Key Laboratory of Time and Frequency Primary Standards, Chinese Academy of Sciences, Xi'an 710600, China
[3] Key Laboratory for Research in Galaxies and Cosmology, Chinese Academy of Sciences, Hefei 230026, China
[4] University of Chinese Academy of Sciences, Beijing 100049, China
[5] Key Laboratory of Precision Navigation and Timing Technology, Chinese Academy of Sciences, Xi'an 710600, China

Received 2015 July 8; accepted 2015 September 11

Abstract Relic gravitational waves (RGWs), a background originating during inflation, would leave imprints on pulsar timing residuals. This makes RGWs an important source for detection of RGWs using the method of pulsar timing. In this paper, we discuss the effects of RGWs on single pulsar timing, and quantitatively analyze the timing residuals caused by RGWs with different model parameters. In principle, if the RGWs are strong enough today, they can be detected by timing a single millisecond pulsar with high precision after the intrinsic red noises in pulsar timing residuals are understood, even though simultaneously observing multiple millisecond pulsars is a more powerful technique for extracting gravitational wave signals. We correct the normalization of RGWs using observations of the cosmic microwave background (CMB), which leads to the amplitudes of RGWs being reduced by two orders of magnitude or so compared to our previous works. We obtained new constraints on RGWs using recent observations from the Parkes Pulsar Timing Array, employing the tensor-to-scalar ratio $r = 0.2$ due to the tensor-type polarization observations of CMB by BICEP2 as a reference value, even though its reliability has been brought into question. Moreover, the constraints on RGWs from CMB and Big Bang nucleosynthesis will also be discussed for comparison.

Key words: gravitational waves: general — pulsars: general — inflation

1 INTRODUCTION

A stochastic background of relic gravitational waves (RGWs) is predicted by applications of both general relativity and quantum mechanics to cosmology (Grishchuk 1975, 2001; Starobinskiĭ 1979; Maggiore 2000; Zhang et al. 2005, 2006; Miao & Zhang 2007; Giovannini 2010). These RGWs are theorized to have originated from quantum fluctuations during the inflationary stage. Hence, RGWs carry unique information about the very early universe and serve as a probe into the universe much earlier than the cosmic microwave background (CMB) can do. As an advantage for their possible detection, RGWs are believed to be spread over a very broad frequency band, $\sim 10^{-19} - 10^{10}$ Hz, which makes them one of the major scientific targets of various types of gravitational wave (GW) detectors, such as ground-based interferometers at $10^2 - 10^3$ Hz (The LIGO Scientific Collaboration & The Virgo Collaboration 2009; Willke et al. 2002; Acernese et al. 2005; Somiya 2012), space-based interferometers at $10^{-4} - 10^{-1}$ Hz (Seto et al. 2001; Crowder & Cornish 2005; Cutler & Harms 2006; Kawamura et al. 2006; Amaro-Seoane et al. 2012), and high-frequency GW detectors around 100 MHz (Cruise 2000; Tong & Zhang 2008; Li et al. 2003, 2008; Tong et al. 2008; Akutsu et al. 2008). For very low frequencies around 10^{-18} Hz, RGWs can be detected by measuring the magnetic type of polarization in CMB (Zaldarriaga & Seljak 1997; Kamionkowski et al. 1997), which has been a detection goal of WMAP (Page et al. 2007; Komatsu et al. 2011; Hinshaw et al. 2013), Planck (Planck Collaboration et al. 2014), and BICEP2 (Ade et al. 2014).

Another important tool to detect RGWs directly is pulsar timing. The existence of a stochastic gravitational wave (GW) background will make the times of arrival (TOAs) of the pulses emitted from pulsars fluctuate. The fluctuations of TOA are implied in the pulsar timing residuals. If multiple millisecond pulsars are observed simultaneously, forming pulsar timing arrays (PTAs) (Detweiler 1979; Romani & Taylor 1983; Hellings & Downs 1983; Kaspi et al. 1994), GW signals can be extracted by correlating the timing residuals of each pair (Detweiler 1979; Jenet et al. 2005). PTAs respond to the frequency range of $10^{-9} - 10^{-6}$ Hz, which is determined by observational characteristics. Currently, there are several such projects operating, such as the Parkes Pulsar Timing Array (PPTA)

(Hobbs 2008; Manchester et al. 2013), European Pulsar Timing Array (EPTA) (van Haasteren et al. 2011), and the North American Nanohertz Observatory for Gravitational Waves (NANOGrav) (Demorest et al. 2013). Much more sensitive facilities like the Five-hundred-meter Aperture Spherical Telescope (FAST) (Nan et al. 2011; Hobbs et al. 2014) and Square Kilometre Array (SKA) (Kramer et al. 2004; Janssen et al. 2015) are being planned or are under construction.

Even though there has been no direct detection of RGWs so far, one can still give constraints on RGWs based on current observations and some conceivable theories. These constraints could prevent us from choosing some unreasonable parameters for RGWs. At present, various constraints on GW background have been studied. Recent observations from PPTA gave an upper limit on the energy density spectrum $\Omega_g(f_{\rm PPTA})$ at $f_{\rm PPTA} = 2.8$ nHz (Shannon et al. 2013). On the other hand, physical processes that happened in the early universe can also provide constraints on RGWs. Big Bang nucleosynthesis (BBN) puts a tight upper bound on the total energy fraction (Maggiore 2000) of GW background for frequencies $f > 10^{-10}$ Hz (Allen & Romano 1999). CMB and matter power spectra also give an upper limit on the total energy fraction of GWs for frequencies $f > 10^{-15}$ Hz (Smith et al. 2006). Therefore, a successful model of RGWs should be compatible with the above constraints. The RGW spectrum is, to a large extent, mainly described by the initial amplitude normalized by the tensor-to-scalar ratio r (Boyle & Steinhardt 2008) and the inflation spectral index β (Grishchuk 2001; Zhang et al. 2005; Miao & Zhang 2007; Tong & Zhang 2009). Here, we assume a zero running spectral index α_t (Tong & Zhang 2009), since it only affects the spectrum at high frequencies. Since β directly describes the expansion behavior of inflation, determination of or constraints on β would be powerful in discriminating various inflationary models. The aforementioned bounds can be converted into constraints on β for a fixed r (Tong & Zhang 2009; Zhang et al. 2010) and for a varying r in a general analysis (Tong et al. 2014). The WMAP observations of spectra associated with CMB anisotropies and polarization have yielded upper bounds on the ratio r of RGWs with a fixed scalar index (Komatsu et al. 2011). Moreover, recent observations of the polarizations of CMB by BICEP2 (Ade et al. 2014) gave what hitherto has been the best estimation: $r = 0.2$. Although this result has been brought into question, we still use $r = 0.2$ as a reference value throughout this paper.

It is worth pointing out that we corrected the normalization of the amplitude of RGWs at a pivot k_0 by using the tensor-type power spectrum of CMB at the time corresponding to the k_0 mode re-entering the Hubble horizon instead of that at the present time. This will reduce the amplitudes of RGWs for all the modes by two orders of magnitude or so compared to our previous works (Tong 2012; Tong et al. 2014). Hence, we will give new constraints on RGWs based on theoretical RGWs and the updated observational data of PPTA. As a general discussion, we will not employ quantum normalization (Grishchuk 2001; Tong et al. 2014) in this paper. Based on these conditions, we will study how RGWs affect pulsar timing with different values of β both in the time domain and the frequency domain. Moreover, we will quantitatively calculate the corresponding pulsar timing residuals induced by RGWs for different β. Even though simultaneously observing multiple millisecond pulsars is a more powerful technique for extracting GW signals, in this paper we only discuss the effect of RGWs on the TOAs of an individual pulsar since it is the basis for GW detection by PTAs. In principle, one can also extract the signal of GWs from timing residuals of a single pulsar with the assumption that the intrinsic red noises are understood. Thus, a comparison between the detection sensitivity curve determined by a ground clock and white-timing noise with the theoretical spectra of RGWs will be given. Throughout this paper we the use units in which the light speed $c = 1$.

2 RELIC GRAVITATIONAL WAVES IN THE ACCELERATING UNIVERSE

In a spatially flat universe, the perturbed Friedmann-Robertson-Walker metric under the existence of the RGWs is

$$ds^2 = a^2(\tau)\Big[-d\tau^2 + (\delta_{ij} + h_{ij})dx^i dx^j\Big], \quad (1)$$

where $a(\tau)$ is the scale factor, τ is the conformal time, and h_{ij} stands for perturbations to the homogenous and isotropic spacetime background due to RGWs. According to the Einstein field equations, RGWs satisfy

$$\partial_\mu\Big[\sqrt{-g}\partial^\mu h_{ij}(\tau, \boldsymbol{x})\Big] = 0\,, \quad (2)$$

where $g \equiv \det(g_{\mu\nu})$. The general solution of Equation (2) can be expanded as k-modes in Fourier space, and has the following form

$$h_{ij}(\tau, \boldsymbol{x}) = \sum_{A=+,\times}\int \frac{d^3\boldsymbol{k}}{(2\pi)^{3/2}}\epsilon^A_{ij}h^A_k(\tau)e^{i\boldsymbol{k}\cdot\boldsymbol{x}}\,, \quad (3)$$

where A stands for the two polarization states under the transverse-traceless gauge. Since the two polarizations of $h^A_k(\tau)$ have the same statistical properties and give equal contributions to the unpolarized RGW background, the summation index A can be dropped. For a power law in the form $a(\tau) \propto \tau^\alpha$, $h_k(\tau)$ has an analytic solution which is a linear combination of Bessel and Neumann functions (Zhang et al. 2005, 2006; Miao & Zhang 2007). In fact, the scale factor in all the stages of cosmic expansion of the universe can be written in forms of a power law (Grishchuk 2001; Miao & Zhang 2007; Tong & Zhang 2009; Tong 2012). For example, the scale factor in the inflationary stage has the following form

$$a(\tau) = l_0|\tau|^{1+\beta}, \quad -\infty < \tau \leq \tau_1, \quad (4)$$

where the inflation index β is a model parameter describing the expansion behavior of inflation, and τ_1 denotes the

end of inflation. The special case of $\beta = -2$ corresponds to the exact de Sitter expansion driven by a constant vacuum energy density. However, for inflationary expansions driven by some dynamic field, the predicted values of β could deviate from -2, depending on specific models. In the single-field slow-roll inflation model, one always has $\beta < -2$, i.e., a red spectrum (Liddle & Lyth 2000). For example, the relation $n_s = 2\beta + 5$ which is often employed (Grishchuk 2001; Tong & Zhang 2009) gives $\beta = -2.02$ for $n_s \simeq 0.96$ based on the observation of CMB by Planck (Planck Collaboration et al. 2014). However, some other inflation models, such as those that incorporate phantom inflation (Piao & Zhang 2004), also predict a blue spectrum, which has not been excluded by observations (Stewart & Brandenberger 2008; Camerini et al. 2008). Below, we recognize β as a major free parameter of RGWs. As shown in Tong (2013), β_s describing the expansion behavior of the reheating process only affects the RGWs at very high frequencies which are far above the upper limit on frequency of the pulsar timing response. In this paper, we will take $\beta_s = 1$ (Starobinsky 1980; Kuroyanagi et al. 2009). After the radiation-dominant stage and the matter-dominant stage, the universe is undergoing an accelerating stage and the scale factor has the following form

$$a(\tau) = l_H|\tau - \tau_a|^{-\gamma}\,, \tag{5}$$

where $\gamma \simeq 3.5$ can be determined by a numerical fitting method with the energy density contrast $\Omega_\Lambda = 0.685$ given by Planck+WMAP (Planck Collaboration et al. 2014). Conveniently, $|\tau_0 - \tau_a| = 1$ was employed (Zhang et al. 2005, 2006), i.e., the present scale factor $a(\tau_0) = l_H$. By definition, one has $l_H = \gamma/H_0$, where the Hubble constant $H_0 = 100\,h$ km s^{-1} Mpc^{-1} with $h = 0.673$ (Planck Collaboration et al. 2014). The coefficients and constants embedded in the expressions of the scale factors can be determined by the continuity of $a(\tau)$ and $a'(\tau)$ at the points joining the various stages.

The increases of the scale factor for different stages are defined as

$$\begin{aligned}
\zeta_1 &\equiv a(\tau_s)/a(\tau_1),\\
\zeta_s &\equiv a(\tau_2)/a(\tau_s),\\
\zeta_2 &\equiv a(\tau_E)/a(\tau_2),\\
\zeta_E &\equiv a(\tau_0)/a(\tau_E),
\end{aligned}$$

where τ_s, τ_2 and τ_E represent the beginnings of the radiation-dominated stage, the matter-dominated stage and the accelerating stage, respectively. For the accelerating stage in the simple ΛCDM model, one has $\zeta_E = 1 + z_E \simeq (\Omega_\Lambda/\Omega_m)^{1/3}$, where z_E is the redshift when the accelerating expansion begins. For the matter-dominated stage, one has $\zeta_2 = (1 + z_{\rm eq})\zeta_E^{-1}$ with $z_{\rm eq} = 3402$ (Planck Collaboration et al. 2014). For the radiation-dominated stage, the value of ζ_s depends on the reheating temperature $T_{\rm RH}$, at which time the radiation-dominated stage begins. Due to conservation of the entropy, ζ_s can be written in terms of $T_{\rm RH}$ (Tong 2012, 2013)

$$\zeta_s = \frac{T_{\rm RH}}{T_{\rm CMB}(1 + z_{\rm eq})}\left(\frac{g_{*s}}{g_{\star s}}\right)^{1/3}, \tag{6}$$

where $T_{\rm CMB} = 2.725\,{\rm K} = 2.348 \times 10^{-13}$ GeV is the present CMB temperature, $g_{*s} \simeq 200$ is the effective number of relativistic species contributing to the entropy after the reheating, and $g_{\star s} = 3.91$ is that after recombination (Watanabe & Komatsu 2006; Tong 2012). For single field inflation, CMB data would yield the lower bound of $T_{\rm RH} \gtrsim 6 \times 10^3$ GeV, and the largest upper bound could be up to $T_{\rm RH} \lesssim 3 \times 10^{15}$ GeV (Martin & Ringeval 2010). Some models like the slow-roll massive scalar field inflation, predict a definite value of $T_{\rm RH} = 5.8 \times 10^{14}$ GeV (Tong 2012). In this paper we generally consider a large range of $T_{\rm RH} \sim (10^4 - 10^{15})$ GeV for a complete demonstration. The uncertainty in $T_{\rm RH}$ is due to the lack of knowledge on the reheating process that happened following the inflationary expansion that converted vacuum energy into radiation, so the parameter ζ_1 is also uncertain. Based on the slow-roll scalar inflation models (Mielczarek 2011; Tong 2012, 2013), ζ_1 depends on the specific form of the potential V that drives the inflation. However, the determination of ζ_1 in that method has a very large relative uncertainty. If we calculate the spectra of RGWs at low frequencies, some particular values of ζ_1 can be set as it only affects RGWs at very high frequencies.

The spectrum of RGWs $h(k,\tau)$ is defined by

$$\langle h^{ij}(\tau,\boldsymbol{x})h_{ij}(\tau,\boldsymbol{x})\rangle \equiv \int_0^\infty h^2(k,\tau)\frac{dk}{k}\,, \tag{7}$$

where the angle brackets mean ensemble average. The present RGW spectrum is related to the *characteristic strain spectrum* (Maggiore 2000) or *chirp amplitude* (Boyle et al. 2006; Boyle & Steinhardt 2008) by $h_c(f) \equiv h(f,\tau_0)/\sqrt{2}$. Assuming that the wave mode crosses the horizon of the universe when $\lambda/(2\pi) = 1/H$, then the characteristic comoving wavenumber at a certain joining time τ_x can be defined as (Tong et al. 2014)

$$k_x \equiv k(\tau_x) = a(\tau_x)H(\tau_x)\,. \tag{8}$$

For example, the characteristic comoving wavenumber at present is $k_H = a(\tau_0)H_0 = \gamma$. By a similar calculation, one has the following relations

$$\frac{k_E}{k_H} = \zeta_E^{-\frac{1}{\gamma}}, \quad \frac{k_2}{k_E} = \zeta_2^{\frac{1}{2}}, \quad \frac{k_s}{k_2} = \zeta_s, \quad \frac{k_1}{k_s} = \zeta_1^{\frac{1}{1+\beta_s}}. \tag{9}$$

In the present universe, the physical frequency is related to a comoving wavenumber k as

$$f = \frac{k}{2\pi a(\tau_0)} = \frac{k}{2\pi l_H}\,. \tag{10}$$

Thus, one can easily have $f_H = H_0/2\pi$, and other characteristic frequencies can be easily determined subsequently by Equation (9). Note that f_s depends on the value of $T_{\rm RH}$.

The present energy density contrast of RGWs is defined by $\Omega_{\rm GW} = \langle\rho_g\rangle/\rho_c$, where ρ_g is the energy density of RGWs and $\rho_c = 3H_0^2/8\pi G$ is the critical energy density. The dimensionless energy density spectrum is related to the characteristic amplitude of RGWs as (Grishchuk 2001; Maggiore 2000)

$$\Omega_g(f) = \frac{d\Omega_{\rm GW}}{d\ln f} = \frac{2\pi^2}{3}h_c^2(f)\Big(\frac{f}{H_0}\Big)^2 . \qquad (11)$$

The analytic solutions of RGWs have been studied by many authors (Zhang et al. 2006; Watanabe & Komatsu 2006; Miao & Zhang 2007; Kuroyanagi et al. 2009; Tong & Zhang 2009). On the other hand, the approximate solutions of RGWs in the whole frequency range were listed in Tong (2012). Even though the initial amplitude of RGWs can, in principle, be given by the quantum normalization condition (Tong et al. 2014), it relies on many physical processes which are not well understood at present. Here, for a simple discussion, we will not consider the normalization condition. On the other hand, the initial amplitude should be normalized to observations. Below, we will determine the initial amplitude of RGWs based on observations of CMB.

3 CONSTRAINTS ON RGWS BY CURRENT OBSERVATIONS

3.1 Determining the Primordial Amplitude of RGWs from Observations of CMB

From observations of the B-mode polarization in the spectrum of CMB, the power spectrum of RGWs at a pivot wavenumber $k_0/a(\tau_0) = 0.002$ Mpc^{-1} can be normalized to the scalar power spectrum using the tensor-to-scalar ratio (Peiris et al. 2003; Spergel et al. 2007; Komatsu et al. 2011)

$$r \equiv \frac{\Delta_h^2(k_0)}{\Delta_{\mathcal{R}}^2(k_0)} , \qquad (12)$$

where $\Delta_h^2(k_0) \equiv h^2(k_0,\tau_i)$ (Boyle & Steinhardt 2008) with τ_i denoting the moment that a mode k re-enters the Hubble horizon, and the scalar power spectrum $\Delta_{\mathcal{R}}^2(k_0) = 2.427\times10^{-9}$ given by WMAP 9+BAO+H_0 (Hinshaw et al. 2013). It is worth pointing out that we used an incorrect normalization in our previous work (Tong 2012; Tong et al. 2014), where $\Delta_h^2(k_0) \equiv h^2(k_0,\tau_0)$ was employed. This overestimated the spectrum of RGWs by two orders of magnitude or so, which will be analyzed later. Recently, the detection of B-mode polarization at degree angular scales in CMB by BICEP2 (Ade et al. 2014) gave a definite value $r = 0.2^{+0.07}_{-0.05}$. Even though this result was subsequently brought into question (BICEP2/Keck and Planck Collaborations et al. 2015), we still take $r = 0.2$ in the following for a tentative demonstration. In addition, CMB observations can also give constraints on the ratio r (Hinshaw et al. 2013; Planck Collaboration et al. 2014; BICEP2/Keck and Planck Collaborations et al. 2015). For example, Planck Collaboration et al. (2014) gave $r < 0.11$ and $r < 0.26$ for a vanishing α_s and a non-vanishing α_s, respectively. The current limit is given by a joint analysis of BICEP2/Keck Array and Planck Data (BICEP2/Keck and Planck Collaborations et al. 2015): $r_{0.05} < 0.12$ at the 95% confidence level. On the other hand, a lower limit $r \gtrsim 10^{-2}$ was obtained (Boyle et al. 2006) using a discrete, model-independent measure of the degree of fine-tuning required, if $0.95 \lesssim n_s < 0.98$, in accord with current measurements.

According to the approximate solutions listed in Tong (2012), the spectrum of RGWs at $f = f_0$ satisfies

$$h(k_0,\tau_0) = A\left(\frac{f_0}{f_H}\right)^{\beta}(1+z_E)^{-\frac{2+\gamma}{\gamma}}, \qquad (13)$$

where A stands for the initial amplitude of RGWs and it can be determined by observations. Equation (13) means that the k_0-mode of RGWs re-entered the horizon at the matter-dominated stage since $f_H < f_0 < f_2$. So, $h(k_0,\tau_0)$ has suffered a decay from the time the k_0-mode re-entered the horizon to the present time, i.e., $h(k_0,\tau_0) = h(k_0,\tau_i)\frac{a(\tau_i)}{a(\tau_0)}$, where $\frac{a(\tau_i)}{a(\tau_0)}$ is the decaying factor. From Equations (9) and (13), one can easily have

$$h(k_0,\tau_i) = A\left(\frac{f_0}{f_H}\right)^{2+\beta} . \qquad (14)$$

Combining Equations (12) and (14), one has

$$A = \sqrt{\Delta_{\mathcal{R}}^2(k_0)r}\left(\frac{f_H}{f_0}\right)^{2+\beta} . \qquad (15)$$

Hence, A can be determined for a given r and β. Figure 1 shows a comparison of the analytic spectrum and the approximate spectrum of RGWs for $T_{\rm RH} = 10^{15}$ GeV, where $\beta = -2$ and $\zeta_1 = 10^5$ were also set. The value of ζ_1 was chosen such that f_1 should be lower than the upper limit on frequency $\sim 4\times10^{10}$ Hz (Grishchuk 2001; Tong 2012). One can see that the approximate spectrum agrees with the analytic spectrum very well, so we can constrain some model parameters using the approximate spectra of RGWs simply from observations. ζ_s depends on $T_{\rm RH}$ linearly, as does f_s as can be seen from Equation (9). We plotted the approximate spectrum for the cases of $T_{\rm RH} = 10^4$ GeV in Figure 1. It is clear that different $T_{\rm RH}$ only affects the spectrum at very high frequencies ($\gtrsim 10^{-3}$ Hz). Since PTAs respond to frequencies localized in the range of $10^{-9} - 10^{-6}$ Hz, the imprints of RGWs on PTAs do not depend on the value of $T_{\rm RH}$.

3.2 Constraints on β by PTAs and the Very Early Universe

PTA experiments have set constraints on the GW background (Bertotti et al. 1983; Kaspi et al. 1994; Thorsett & Dewey 1996; McHugh et al. 1996; Jenet et al. 2006; Hobbs et al. 2009; van Haasteren et al. 2011; Demorest et al. 2013;

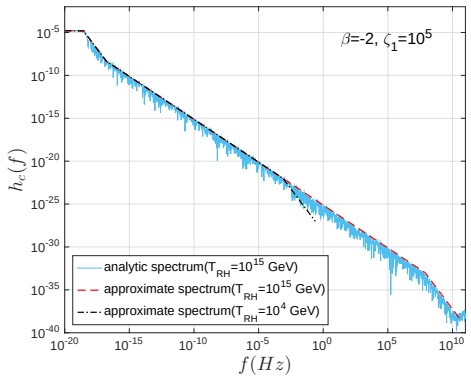

Fig. 1 A comparison between the analytic (*solid line*) and approximate (*dashed line*) spectra of RGWs with a fixed parameter set of $\beta = -2$, $\zeta_1 = 10^{-5}$ and $T_{\rm RH} = 10^{15}$ GeV. An approximate spectrum (*dot-dashed line*) of RGWs with $T_{\rm RH} = 10^4$ GeV is also plotted for comparison.

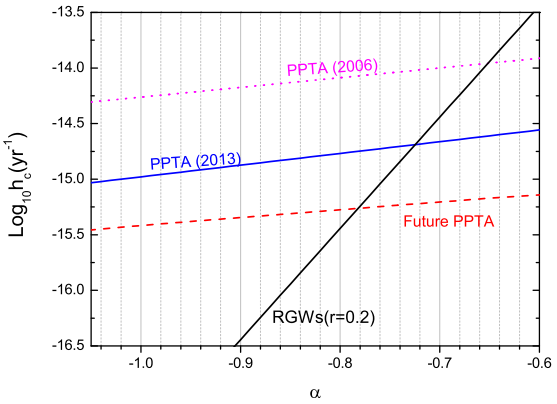

Fig. 2 The constraints on α given by the PPTA (2006) (Jenet et al. 2006), PPTA (2013) (Shannon et al. 2013) and values from the PPTA expected in the future (Jenet et al. 2006), calculated by confronting RGWs with $r = 0.2$. These constraints are made at the frequency of one cycle per year.

Zhao et al. 2013). In the data analysis of PTAs, the characteristic strain spectrum of GW background is usually modeled with a power law in the form

$$h_c(f) = h_{\rm yr}\left(\frac{f}{\rm yr^{-1}}\right)^{\alpha}, \tag{16}$$

where $h_{\rm yr}$ is the amplitude at $f = {\rm yr}^{-1}$. For the frequency band $10^{-9} \leq f \leq 10^{-6}$ Hz of PTA experiments, the characteristic strain spectrum has the following form (Tong 2012)

$$h_c(f) = \frac{A}{\sqrt{2}}\left(\frac{f}{f_H}\right)^{1+\beta}\left(\frac{f_H}{f_2}\right)(1+z_E)^{-\frac{2+\gamma}{\gamma}}. \tag{17}$$

With the help of Equation (15), Equation (17) can be rewritten as

$$h_c(f) = \sqrt{\frac{\Delta^2_{\mathcal{R}}(k_0)r}{2}}\left(\frac{f_H^2}{f_0 f_2}\right)\left(\frac{f}{f_0}\right)^{1+\beta}(1+z_E)^{-\frac{2+\gamma}{\gamma}}. \tag{18}$$

Note that $f/f_0 \gg 1$ in the pulsar timing frequency band. Comparing Equation (16) and Equation (18) tells us that the power law index is related to the inflation index via

$$\alpha = 1 + \beta. \tag{19}$$

Improving on earlier work (e.g. Kaspi et al. 1994), Jenet et al. (2006) developed a frequentist technique in statistics, and have calculated an upper limit on $h_{\rm yr}$ for different values of α. Recently, Shannon et al. (2013) provided an upper limit of $h_{\rm yr} < 2.4 \times 10^{-15}$ at the 95% confidence level for $\alpha = -2/3$ using data from PPTA and available observations from the Arecibo Observatory. Even though this limit is intended for supermassive black hole binaries, one can equivalently translate it to the case of RGWs, which leads to $h_{\rm yr} < 1.0 \times 10^{-15}$ for $\alpha = -1$. Note that these limits are independent of H_0.

Figure 2 displays the upper limit curves of $h_{\rm yr}(\alpha)$ for PPTA in different phases. The values provided by PPTA (2006) and those expected in the future as obtained from simulated data with 20 possible pulsars using PPTA timing are taken from Jenet et al. (2006). To constrain the parameter α, $h_c({\rm yr}^{-1})$ with $r = 0.2$ is also plotted. As shown in Tong et al. (2014), the condition $h_c({\rm yr}^{-1}) < h_{\rm yr}(\alpha)$ leads to an upper limit on α (or β) for a given r. Since $r = 0.2$ is set in this paper, PPTA (2013) provides an upper limit of $\alpha < -0.70$ ($\beta < -1.70$). Comparably, PPTA (2006) gives an upper limit of $\alpha < -0.63$ ($\beta < -1.63$), and future PPTA observations will allow an upper limit of $\alpha < -0.76$ ($\beta < -1.76$).

Besides the constraints from PTAs, some other observations also give constraints on RGWs. For example, β can be constrained by ground-based laser interferometers (Tong & Zhang 2009; Chen et al. 2014). However, ground-based laser interferometers respond to RGWs at the frequency range of $10^2 - 10^3$ Hz, and RGWs with high frequencies depending on theoretical models which are not well understood. For instance, if we choose $T_{\rm RH} = 10^4$ GeV, there will be no RGWs with frequencies larger than 0.24 Hz. In addition, BBN and CMB can give constraints on the GW energy density contrast at the time of nucleosynthesis and CMB decoupling, respectively. The constraint from BBN is given by $\Omega_{\rm GW}^{\rm BBN} < 1.1 \times 10^{-5}(N_\nu - 3)$ (Maggiore 2000), where the effective number of neutrino species at the time of BBN has an upper bound of $N_\nu - 3 < 1.4$ (Cyburt et al. 2005). On the other hand, CMB gives $\Omega_{\rm GW}^{\rm CMB} < 1.3 \times 10^{-5}$ (Smith et al. 2006). Note that the lower frequency limits contributing the energy density contrasts for BBN and CMB are different. For BBN, $f_{\rm low} \sim 10^{-10}$ Hz corresponds to the horizon scale at the time of BBN (Allen & Romano 1999); while for CMB, $f_{\rm low} \sim 10^{-15}$ corresponds to the horizon scale at the decoupling of CMB (Zhang et al. 2010). However, the upper limit on frequency for both of the two cases is f_1. As pointed out above, f_1 depends on ζ_s and thus depends on

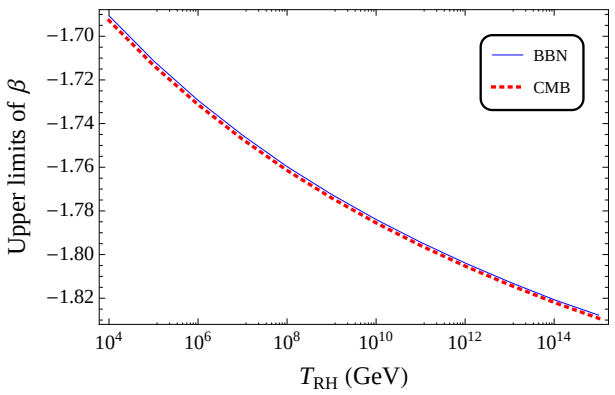

Fig. 3 Upper limits on β with varying $T_{\rm RH}$ given by BBN and CMB.

$T_{\rm RH}$ in turn, so the constraints on β given by BBN or CMB depend on $T_{\rm RH}$. As shown in Equation (9), f_1 also depends on ζ_1, however, we found that the limits of β constrained by BBN/CMB are nearly independent of ζ_1. This can be explained because ζ_1 only affects the power spectrum in the frequency band (f_s, f_1), which contributes very little to the total energy density contrast. This was also clearly demonstrated in figure 1 of Tong et al. (2014).

Figure 3 shows the upper limits on β constrained by BBN and CMB with varying $T_{\rm RH}$. One can see that BBN and CMB define almost the same constraints for the whole range of $T_{\rm RH}$. The most stringent constraint is given by $\beta < -1.83$ with $T_{\rm RH} = 10^{15}$ GeV, which is more stringent than those given by current PPTA data. However, one should bear in mind that constraints on β given by PTAs are independent of $T_{\rm RH}$.

4 IMPRINTS OF RGWS ON PULSAR TIMING

The existence of GWs will change the geodesic of photons from millisecond pulsars as they travel to the observer. Consequently, the TOAs of the electromagnetic signals from pulsars will be perturbed, forming the so-called timing residuals if the effect of RGWs is not taken into account in the timing model. The GW background would lead to a red power law spectrum of the timing residuals. Even though such red spectra can also be produced by intrinsic noise of pulsars (Verbiest et al. 2009; Shannon & Cordes 2010), inaccuracies in the solar system ephemeris (Champion et al. 2010) or variations in terrestrial time standards (Hobbs et al. 2012), a GW background produces a unique signature in the timing residuals that can be confirmed by observing correlated signals between multiple pulsars widely distributed on the sky (Hellings & Downs 1983; Jenet et al. 2005). However, here we only analyze how RGWs affect the timing residuals of a single pulsar. In principle, if the GW signals are strong enough, one could extract their signals buried in the data of the timing residual measurements after all known effects have been accounted for. On the other hand, even though GWs are very weak, one can still constrain the amplitude of GWs with the long-term accumulation of data in the form of timing residuals.

The frequency of the signals from a pulsar will be shifted due to the existence of a GW. For a GW propagating in the direction $\hat{\Omega}$, the redshift of the signals from a pulsar in the direction $\hat{p}$ is given by (Detweiler 1979; Anholm et al. 2009)

$$z(t,\hat{\Omega}) = \frac{\nu_e - \nu_p}{\nu_p} = \frac{\hat{p}^i\hat{p}^j}{2(1+\hat{\Omega}\cdot\hat{p})}\Delta h_{ij}\,, \qquad (20)$$

where ν_e and ν_p represent the frequencies of the pulse received at the Earth and the pulse emitted at the pulsar, respectively, and

$$\Delta h_{ij} = [h_{ij}(t_p,\hat{\Omega}) - h_{ij}(t_e,\hat{\Omega})]\,, \qquad (21)$$

is the difference in the metric perturbation traveling along the direction $\hat{\Omega}$ at the pulsar compared to that at the Earth. t_p and t_e are the times at which the GW passes the pulsar and the Earth, respectively. Note that the standard Einstein summation convention was used in Equation (20). The vectors $(t_e, \boldsymbol{x}_e)$ and $(t_p, \boldsymbol{x}_p)$ give the spacetime coordinates of the Solar System barycenter (SSB) and the pulsar, respectively. In the following, we choose a coordinate system where the origin of the space coordinates is located at the SSB, and use t instead of t_e to denote the time coordinate. Moreover, the following conventions are often used (Anholm et al. 2009),

$$t_p = t - L\,, \quad \boldsymbol{x}_p = L\hat{p}\,, \qquad (22)$$

where L is the distance of the pulsar from the SSB. If we assume that the amplitude of the GW is the same at the SSB and the pulsar, then Δh_{ij} can be written as the following in the form of a Fourier integration (Anholm et al. 2009)

$$\Delta h_{ij}(t,\hat{\Omega}) = \sum_{A=+,\times}\int_{-\infty}^{\infty} df e^{i2\pi ft}(e^{-i2\pi fL(1+\hat{\Omega}\cdot\hat{p})} - 1)h_A(f,\hat{\Omega})\epsilon_{ij}^A(\hat{\Omega})\,, \qquad (23)$$

where A stands for the two polarizations of GWs, and the corresponding tensor $\epsilon_{ij}^A(\Omega)$ can be written as

$$\epsilon_{ij}^+(\hat{\Omega}) = \hat{m}_i\hat{m}_j - \hat{n}_i\hat{n}_j, \quad \epsilon_{ij}^\times(\hat{\Omega}) = \hat{m}_i\hat{n}_j + \hat{n}_i\hat{m}_j\,, \qquad (24)$$

with $\hat{m}$ and $\hat{n}$ being unit vectors that are orthogonal to $\hat{\Omega}$ and to each other. One has straightforwardly,

$$\epsilon_{ij}^A(\hat{\Omega})\epsilon^{A',ij}(\hat{\Omega}) = 2\delta^{AA'}\,. \qquad (25)$$

If we assume that the stochastic background is isotropic, unpolarized and stationary, the ensemble average of the Fourier amplitudes can be written as

$$\langle\tilde{h}_A^*(f,\hat{\Omega})\tilde{h}_{A'}(f',\hat{\Omega}')\rangle = \frac{1}{16\pi}\delta(f-f')\delta^2(\hat{\Omega},\hat{\Omega}')\delta_{AA'}S_h(f)\,. \qquad (26)$$

Note that the spectral density $S_h(f)$ defined above is twice as much as that shown in equation (8) of Maggiore (2000), and satisfies $S_h(f) = S_h(-f)$. Here $S_h(f)$ is called a *one-sided spectral density*, and it is related to the characteristic strain amplitude as (Maggiore 2000)

$$h_c^2(f) = f S_h(f)\,. \tag{27}$$

Substituting Equation (23) into Equation (20), one has

$$z(t,\hat{\Omega}) = \sum_A \int_{-\infty}^{\infty} df e^{i2\pi ft}(e^{-i2\pi fL(1+\hat{\Omega}\cdot\hat{p})} - 1) h_A(f,\hat{\Omega})F^A(\hat{\Omega})\,, \tag{28}$$

where

$$F^A(\hat{\Omega}) \equiv \epsilon_{ij}^A(\hat{\Omega})\frac{1}{2}\frac{\hat{p}^i\hat{p}^j}{1+\hat{\Omega}\cdot\hat{p}} \tag{29}$$

has been defined. For a stochastic GW background, the total redshift is given by summing over the contributions coming from GWs in every direction (Anholm et al. 2009)

$$z(t) = \int_{S^2} d\hat{\Omega}\, z(t,\hat{\Omega})\,. \tag{30}$$

The pulsar timing residual is defined as the integral of the redshift

$$R(t) \equiv \int_0^t dt' z(t')\,. \tag{31}$$

The total relative frequency changes can be divided into two parts

$$s(t) = z(t) + n(t)\,, \tag{32}$$

where $z(t)$ is induced by the RGWs and $n(t)$ is the intrinsic noise in the timing measurement which is assumed to be stationary and Gaussian. In addition, we also assume that

$$\langle z(t)\rangle = \langle n(t)\rangle = 0, \quad \langle z(t)n(t)\rangle = 0\,, \tag{33}$$

where the angle brackets denote the expected value. With the help of Eqs. (26), (28) and (30), the variance of the relative frequency changes is given by

$$\langle z^2(t)\rangle \equiv \int_0^\infty df S_z(f) = F\int_0^\infty df S_h(f)\,, \tag{34}$$

where $S_z(f) = F S_h(f)$ and

$$F \equiv \frac{1}{8\pi}\int_{S^2} d\hat{\Omega}\Big|e^{i2\pi fL(1+\hat{\Omega}\cdot\hat{p})} - 1\Big|^2 \sum_A F^A(\hat{\Omega})F^A(\hat{\Omega})\,. \tag{35}$$

Using the definition in Equation (29), one can easily obtain (Jenet et al. 2011)

$$F = \frac{1}{3} - \frac{1}{8\pi^2 f^2 L^2} + \frac{\sin(4\pi fL)}{32\pi^3 f^3 L^3}\,. \tag{36}$$

The behavior of F is shown in Figure 4. It can be seen that F is generally frequency-dependent, however, F will converge to a fixed value of $1/3$ when $fL \gtrsim 3$. For pulsar timing experiments, the distances of millisecond pulsars are usually larger than 0.1 kpc, and $fL > 10$ for frequencies $f > 10^{-9}$ Hz. Therefore, one always has $F = 1/3$ for pulsar timing experiments. The factor F represents the root mean square (rms) signal response averaged over the sky and polarization states.

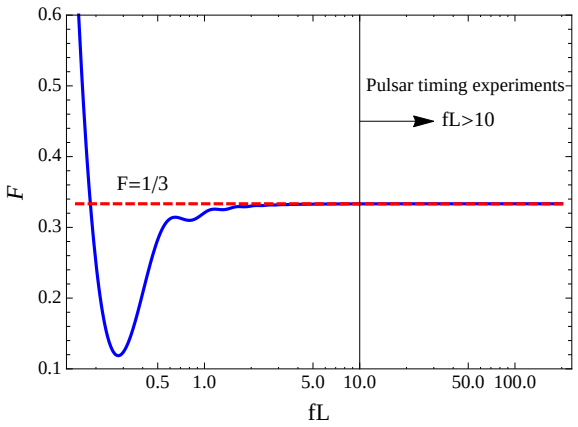

Fig. 4 The property of the reduction factor F with different regimes of fL. For the pulsar timing experiments, one has $fL > 10$.

Similarly, the ensemble average of the Fourier components of the noise satisfies

$$\langle \tilde{n}^*(f)\tilde{n}(f')\rangle = \frac{1}{2}\delta(f-f')S_n(f)\,, \tag{37}$$

where the noise spectral density satisfies $S_n(f) = S_n(-f)$ with dimension Hz^{-1}. So, the variance of the noise is

$$\langle n^2(t)\rangle = \int_0^\infty df S_n(f)\,. \tag{38}$$

Equivalently, the noise level of a GW detector is usually measured by the *strain sensitivity* $\tilde{h}(f) \equiv \sqrt{S_n(f)}$ with dimension $\mathrm{Hz}^{-1/2}$. For a given signal-to-noise ratio (SNR), one can discuss the ability of a detector to reach the minimum detectable amplitude of RGWs. Under the assumption that the dispersion caused by interplanetary plasma is adequately calibrated and the intrinsic rotation instability of the pulsar can be negligible or be well understood, the noise spectrum is characterized by contribution due to the ground clock and a white-timing noise of 100 ns in a Fourier band of $+/-0.5$ cycles/day (Alves & Tinto 2011). The 100 ns level is the current timing goal of PTAs and three pulsars are being timed to this level (Verbiest et al. 2009). Following the noise model discussed in Jenet et al. (2011), the expression for the noise spectral density of the relative frequency fluctuations is (Alves & Tinto 2011)

$$S_{zn}(f) = [4.0\times10^{-31}f^{-1} + 3.41\times10^{-8}f^2]\ \mathrm{Hz}^{-1}\,. \tag{39}$$

For SNR=1, i.e., $S_z(f)/S_{zn}(f) = 1$, we plotted the strain sensitivity for the detection of the GW background by a single pulsar and the analytic strain amplitude per root Hz (considering the F factor) of RGWs, $h_c(f)\sqrt{F/f}$ (Zhang et al. 2010), with different values of β in Figure 5. One can

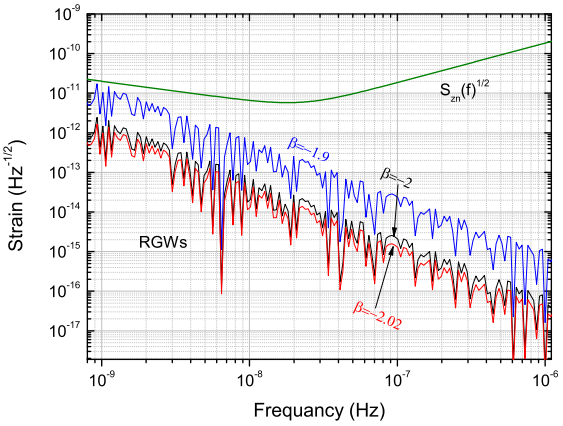

Fig. 5 The strain sensitivity curve to be explored by the noise spectrum of the relative frequency fluctuations for a single pulsar timing. Values for $h_c(f)\sqrt{F/f}$ of RGWs with different parameters $\beta = -1.9$, $\beta = -2.0$ and $\beta = -2.02$ are also demonstrated for comparison.

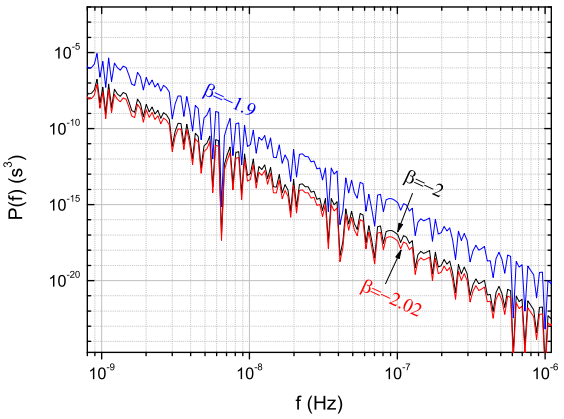

Fig. 6 The one-sided power spectra of the induced timing residuals by RGWs with different β.

see that it is hard to detect RGWs even for a blue spectrum by timing an individual pulsar, however, it is more hopeful that the lower frequencies of RGWs can be detected. Note that SNR=5 is conventionally taken as a detection threshold for PTAs. Thus, the sensitivity curve shown in Figure 5 should be multiplied by a factor of $\sqrt{5}$. Therefore, significant SNR improvements in pulsar timing sensitivities for radio telescopes will be required for reliable detection. There are two methods that can be applied to this type of target. First, one can simultaneously measure the timings of several pulsars. The SNR can be improved by correlating the data of several pulsars just as in the method used in the networks of ground-based interferometers. Second, one should try to suppress various types of noise in the timing measurements.

The one-sided power spectrum of the induced timing residuals by RGWs, $P(f)$, is defined as (Jenet et al. 2006)

$$\int_0^\infty P(f)df = \sigma^2\,, \tag{40}$$

where σ^2 is the variance of the timing residuals generated by the stochastic background of RGWs. The power spectrum $P(f)$ is related to the characteristic strain as

$$P(f) = \frac{1}{12\pi}\frac{1}{f^3}h_c(f)^2. \tag{41}$$

$P(f)$ has the unit of s^3.

Figure 6 shows the corresponding one-sided power spectra of the induced timing residuals by RGWs with $\beta = -1.9$, $\beta = -2$ and $\beta = -2.02$. It can be seen that RGWs with $\beta = -1.9$ lead to a higher $P(f)$ by about two orders of magnitude than that given by RGWs with $\beta = -2$. For $\beta = -1.9$, the power spectrum is as high as 10^{-5} s^3 around 10^{-9} Hz. In fact, the limits of integration are determined by the observing strategy that is used. The lowest detectable frequency is given by $1/T$, where T is the total time span of the data set. The highest one is determined by the Nyquist sampling rate. If one observes pulsars at an interval of Δt, then the highest frequency is $2/\Delta t$. For the observation of pulsar timing, Δt is typically two weeks, and the total timespan for the data is assumed to be around 10 years. Then, based on Equation (40), one has the standard deviation of the timing residuals $\sigma = 3.2$ ns, 0.4 ns and 0.3 ns for $\beta = -1.9$, -2 and -2.02, respectively. For comparison, we also calculated the case of $\beta = -1.8$ with $\sigma = 26.2$ ns, even though β is not possibly so large.

5 SUMMARY

In summary, we analyzed the effects of RGWs on pulsar timing residuals, based on some reasonable parameters constrained by the recent observations of PPTA and physical processes that happened in the very early universe. First of all, we corrected the normalization of RGWs by the CMB observations, and now the spectra are reduced by two orders of magnitude compared to our previous results. Then, we compared the analytic spectrum and the approximate spectrum of RGWs, and we found they matched each other very well. Therefore, one can take advantage of both of them. When we constrain the parameter β by the PPTA, the approximate spectrum is applied in a simple way. However, when we calculate the total energy density contrast and timing residuals induced by RGWs, the analytic spectrum is used. The current PPTA gives a constraint, $\beta < -1.70$, and the future PPTA would give a constraint $\beta < -1.76$. On the other hand, the constraints of β from the BBN/CMB are dependent on some other cosmic parameters, such as the temperature of the reheating process $T_{\rm RH}$ and the expansion times of the reheating process ζ_1. The strongest constraint from BBN/CMB is $\beta < -1.83$. Note that the constraints from BBN/CMB are slightly overestimated because of the effects of neutrino free-streaming (Weinberg 2004), e^+e^- annihilation

and the QCD transition (Schwarz 1998; Wang et al. 2008). It is worth pointing out that constraints on β from the PPTA are more convincing since β is independent of other parameters.

Based on these constraints, we chose $\beta = -1.9$, $\beta = -2$ and $\beta = -2.02$ for demonstration. We compared the sensitivity curve determined by the ground clock and a white noise of 100 ns with the predicted RGWs. It was found that RGWs cannot be detected by a single pulsar timing at present, however, it is very hopeful that RGWs with frequencies as low as 10^{-9} Hz could be detected if the intrinsic red noises were understood. Note that the noise spectrum discussed in this paper is quite ideal, since many other noise components are not included. We quantitatively calculated the rms residuals induced by RGWs with different values of β, and found that the rms residuals are $\sigma = 3.2$ ns, 0.4 ns and 0.3 ns for $\beta = -1.9$, -2 and -2.02, respectively. Moreover, the rms residual can be as much as 26.2 ns for $\beta = -1.8$. In addition, we also showed the power spectra of the induced timing residuals by RGWs with different values of β.

RGWs are a very important and effective tool to exploit knowledge about the very early universe. All the aforementioned constraints on RGWs will help us to understand the early universe more clearly. For example, the parameters describing expansion times of the reheating process ζ_1, the expansion times ζ_s of the radiation-dominated stage and some other parameters can be more accurate. However, quantum normalization is not employed here in order to give a general result, but it should be considered elsewhere for a more complete discussion. Moreover, RGWs play a key role in connecting the subject of cosmology with pulsar timing observations.

Acknowledgements This work was supported by the National Natural Science Foundation of China (Grant Nos. 11103024, 11373028 and 11403030), the Science and Technology Research Development Program of Shaanxi Province, the CAS "Light of West China" Program, and the Open Project of Key Laboratory for Research in Galaxies and Cosmology, Chinese Academy of Sciences (Grant No. 14010205).

References

Acernese, F., Amico, P., Al-Shourbagy, M., et al. 2005, Classical and Quantum Gravity, 22, 869

Ade, P. A. R., Aikin, R. W., Barkats, D., et al. 2014, Physical Review Letters, 112, 241101

Akutsu, T., Kawamura, S., Nishizawa, A., et al. 2008, Physical Review Letters, 101, 101101

Allen, B., & Romano, J. D. 1999, Phys. Rev. D, 59, 102001

Alves, M. E. D. S., & Tinto, M. 2011, Phys. Rev. D, 83, 123529

Amaro-Seoane, P., Aoudia, S., Babak, S., et al. 2012, Classical and Quantum Gravity, 29, 124016

Anholm, M., Ballmer, S., Creighton, J. D. E., Price, L. R., & Siemens, X. 2009, Phys. Rev. D, 79, 084030

Bertotti, B., Carr, B. J., & Rees, M. J. 1983, MNRAS, 203, 945

BICEP2/Keck and Planck Collaborations, Ade, P. A. R., Aghanim, N., et al. 2015, Physical Review Letters, 114, 101301

Boyle, L. A., & Steinhardt, P. J. 2008, Phys. Rev. D, 77, 063504

Boyle, L. A., Steinhardt, P. J., & Turok, N. 2006, Physical Review Letters, 96, 111301

Camerini, R., Durrer, R., Melchiorri, A., & Riotto, A. 2008, Phys. Rev. D, 77, 101301

Champion, D. J., Hobbs, G. B., Manchester, R. N., et al. 2010, ApJ, 720, L201

Chen, J.-W., Zhang, Y., Zhao, W., & Tong, M.-L. 2014, arXiv:1410.7151

Crowder, J., & Cornish, N. J. 2005, Phys. Rev. D, 72, 083005

Cruise, A. M. 2000, Classical and Quantum Gravity, 17, 2525

Cutler, C., & Harms, J. 2006, Phys. Rev. D, 73, 042001

Cyburt, R. H., Fields, B. D., Olive, K. A., & Skillman, E. 2005, Astroparticle Physics, 23, 313

Demorest, P. B., Ferdman, R. D., Gonzalez, M. E., et al. 2013, ApJ, 762, 94

Detweiler, S. 1979, ApJ, 234, 1100

Giovannini, M. 2010, PMC Physics A, 4, 1

Grishchuk, L. P. 1975, Soviet Journal of Experimental and Theoretical Physics, 40, 409

Grishchuk, L. P. 2001, in Lecture Notes in Physics, Berlin Springer Verlag, 562, Gyros, Clocks, Interferometers ...: Testing Relativistic Gravity in Space, eds. C. Lämmerzahl, C. W. F. Everitt, & F. W. Hehl, 167

Hellings, R. W., & Downs, G. S. 1983, ApJ, 265, L39

Hinshaw, G., Larson, D., Komatsu, E., et al. 2013, ApJS, 208, 19

Hobbs, G. 2008, Classical and Quantum Gravity, 25, 114032

Hobbs, G., Jenet, F., Lee, K. J., et al. 2009, MNRAS, 394, 1945

Hobbs, G., Coles, W., Manchester, R. N., et al. 2012, MNRAS, 427, 2780

Hobbs, G., Dai, S., Manchester, R. N., et al. 2014, arXiv:1407.0435

Janssen, G., Hobbs, G., McLaughlin, M., et al. 2015, Advancing Astrophysics with the Square Kilometre Array (AASKA14), 37 (arXiv:1501.00127)

Jenet, F. A., Hobbs, G. B., Lee, K. J., & Manchester, R. N. 2005, ApJ, 625, L123

Jenet, F. A., Hobbs, G. B., van Straten, W., et al. 2006, ApJ, 653, 1571

Jenet, F. A., Armstrong, J. W., & Tinto, M. 2011, Phys. Rev. D, 83, 081301

Kamionkowski, M., Kosowsky, A., & Stebbins, A. 1997, Phys. Rev. D, 55, 7368

Kaspi, V. M., Taylor, J. H., & Ryba, M. F. 1994, ApJ, 428, 713

Kawamura, S., Nakamura, T., Ando, M., et al. 2006, Classical and Quantum Gravity, 23, 125

Komatsu, E., Smith, K. M., Dunkley, J., et al. 2011, ApJS, 192, 18

Kramer, M., Backer, D. C., Cordes, J. M., et al. 2004, New

Astron. Rev., 48, 993
Kuroyanagi, S., Chiba, T., & Sugiyama, N. 2009, Phys. Rev. D, 79, 103501
Li, F.-Y., Tang, M.-X., & Shi, D.-P. 2003, Phys. Rev. D, 67, 104008
Li, F., Baker, Jr., R. M. L., Fang, Z., Stephenson, G. V., & Chen, Z. 2008, European Physical Journal C, 56, 407
Liddle, A. R., & Lyth, D. H. 2000, Cosmological Inflation and Large-Scale Structure, eds. Andrew R. Liddle, & David H. Lyth (Cambridge: Cambridge Univ. Press)
The LIGO Scientific Collaboration & The Virgo Collaboration 2009, Nature, 460, 990
Maggiore, M. 2000, Phys. Rep., 331, 283
Manchester, R. N., Hobbs, G., Bailes, M., et al. 2013, PASA, 30, 17
Martin, J., & Ringeval, C. 2010, Phys. Rev. D, 82, 023511
McHugh, M. P., Zalamansky, G., Vernotte, F., & Lantz, E. 1996, Phys. Rev. D, 54, 5993
Miao, H. X., & Zhang, Y. 2007, Phys. Rev. D, 75, 104009
Mielczarek, J. 2011, Phys. Rev. D, 83, 023502
Nan, R., Li, D., Jin, C., et al. 2011, International Journal of Modern Physics D, 20, 989
Page, L., Hinshaw, G., Komatsu, E., et al. 2007, ApJS, 170, 335
Peiris, H. V., Komatsu, E., Verde, L., et al. 2003, ApJS, 148, 213
Piao, Y.-S., & Zhang, Y.-Z. 2004, Phys. Rev. D, 70, 063513
Planck Collaboration, Ade, P. A. R., Aghanim, N., et al. 2014, A&A, 571, A16
Romani, R. W., & Taylor, J. H. 1983, ApJ, 265, L35
Schwarz, D. J. 1998, Modern Physics Letters A, 13, 2771
Seto, N., Kawamura, S., & Nakamura, T. 2001, Physical Review Letters, 87, 221103
Shannon, R. M., & Cordes, J. M. 2010, ApJ, 725, 1607
Shannon, R. M., Ravi, V., Coles, W. A., et al. 2013, Science, 342, 334
Smith, T. L., Pierpaoli, E., & Kamionkowski, M. 2006, Physical Review Letters, 97, 021301
Somiya, K. 2012, Classical and Quantum Gravity, 29, 124007
Spergel, D. N., Bean, R., Doré, O., et al. 2007, ApJS, 170, 377
Starobinskiĭ, A. A. 1979, Soviet Journal of Experimental and Theoretical Physics Letters, 30, 682
Starobinsky, A. A. 1980, Physics Letters B, 91, 99
Stewart, A., & Brandenberger, R. 2008, J. Cosmol. Astropart. Phys., 8, 12
Thorsett, S. E., & Dewey, R. J. 1996, Phys. Rev. D, 53, 3468
Tong, M. 2012, Classical and Quantum Gravity, 29, 155006
Tong, M. 2013, Classical and Quantum Gravity, 30, 055013
Tong, M.-L., & Zhang, Y. 2008, ChJAA (Chin. J. Astron. Astrophys.), 8, 314
Tong, M. L., Zhang, Y., & Li, F. Y. 2008, Phys. Rev. D, 78, 024041
Tong, M. L., & Zhang, Y. 2009, Phys. Rev. D, 80, 084022
Tong, M. L., Zhang, Y., Zhao, W., et al. 2014, Classical and Quantum Gravity, 31, 035001
van Haasteren, R., Levin, Y., Janssen, G. H., et al. 2011, MNRAS, 414, 3117
Verbiest, J. P. W., Bailes, M., Coles, W. A., et al. 2009, MNRAS, 400, 951
Wang, S., Zhang, Y., Xia, T. Y., & Miao, H. X. 2008, Phys. Rev. D, 77, 104016
Watanabe, Y., & Komatsu, E. 2006, Phys. Rev. D, 73, 123515
Weinberg, S. 2004, Phys. Rev. D, 69, 023503
Willke, B., Aufmuth, P., Aulbert, C., et al. 2002, Classical and Quantum Gravity, 19, 1377
Zaldarriaga, M., & Seljak, U. 1997, Phys. Rev. D, 55, 1830
Zhang, Y., Yuan, Y., Zhao, W., & Chen, Y.-T. 2005, Classical and Quantum Gravity, 22, 1383
Zhang, Y., Er, X. Z., Xia, T. Y., Zhao, W., & Miao, H. X. 2006, Classical and Quantum Gravity, 23, 3783
Zhang, Y., Tong, M. L., & Fu, Z. W. 2010, Phys. Rev. D, 81, 101501 (R)
Zhao, W., Zhang, Y., You, X.-P., & Zhu, Z.-H. 2013, Phys. Rev. D, 87, 124012